Changes in the Isotropic Shielding of the ^{17}O Nucleus upon Torsion in Terminal Oxygen Systems: A Computational Study on Their Origin

Heidi M. Muchall†

Centre for Research in Molecular Modeling and Department of Chemistry and Biochemistry, Concordia University, Montreal, Quebec, H4B 1R6, Canada

Received: May 27, 2008; Revised Manuscript Received: July 14, 2008

We are presenting a computational study on the isotropic shielding, charge, and orbital contributions to the shielding of oxygen in benzaldehydes (Ar−CHO), nitrobenzenes (Ar−NO_2), phenyl isocyanates (Ar−NCO), anilides (Ar−$NHCOCH_3$), and *N*-sulfinylamines (Ar−NSO). In particular, changes upon ortho substitution of the aromatic ring and upon torsion of the unsubstituted parent molecules are examined. The experimentally observed changes in ^{17}O chemical shift, be they upfield or downfield, upon substitution by ortho-alkyl groups are reproduced well by the calculations. Relaxed torsional scans of the parent systems reveal that (a) charges change as expected from resonance arguments and (b) changes in isotropic shielding are monotonic and in line with changes upon substitution, with *N*-sulfinylaniline as an exception. In general, the changes in isotropic shieldings are explained in terms of changes in molecular orbitals, their energies, and relative alignments, whose mixing is magnetically active. Thus, for example, the observed deshielding of ^{17}O upon methyl substitution and upon torsion of benzaldehyde is mainly caused by a contribution from the π-type oxygen lone pair, yet how these contributions change is fundamentally different. As a consequence, the experimentally observed downfield shift upon methyl substitution cannot be interpreted to imply a change in torsion angle between the phenyl ring and the aldehyde group. For *N*-sulfinylaniline, the consecutive downfield shifts upon methyl and *tert*-butyl substitution and the associated changes in torsion angle are in contrast to the 45° maximum in isotropic shielding that is determined from a relaxed torsional scan.

1. Introduction

During the course of our studies on ^{17}O NMR spectra of *N*-sulfinylaniline (Ph−NSO), its substituted derivatives, and their complexes, it became clear that we needed information on the torsional dependence of the ^{17}O chemical shift. Fortunately, it is known that ^{17}O is a good reporter nucleus for conformational changes in aromatic compounds that bear substituents with terminal oxygen atoms,[1] and so such information is readily available for a multitude of functional groups that are more or less obviously related to *N*-sulfinylanilines, such as aromatic isocyanates[2] (Ar−NCO) and amides[3] (acetanilides, Ar−$NHCOCH_3$), aldehydes[4] (Ar−CHO) and nitro compounds[5] (Ar−NO_2). For all of these, molecules with an unsubstituted phenyl ring are planar in gas or liquid phases (even though this might not be the case for the crystal),[3,6] and twisting is traditionally achieved through ortho substitution with groups of increasing steric bulk. In order not to introduce major electronic effects through substitution, methyl, isopropyl, and *tert*-butyl are usually the alkyl groups of choice.

Interestingly, the steric influence on the ^{17}O chemical shift manifests itself in two opposing outcomes. While the ^{17}O nucleus in aromatic isocyanates and in acetanilides is shielded (upfield shift) with increasing bulk in ortho position,[2,3] it is deshielded (downfield shift) in aromatic aldehydes and nitro compounds.[4,5] Upon alkyl substitution in ortho position, the deshielding in aromatic aldehydes and nitro compounds and the shielding in acetanilides have been explained through resonance effects. Thus, in aromatic aldehydes (Chart 1) and nitro compounds, the X═O bond is one (single) bond removed from the aromatic system, and steric inhibition of resonance leads to twisting about this bond and therefore decreased delocalization,[7] increased double bond character,[2] and decreased charge density on oxygen.[1] The same argument, steric inhibition of resonance, leads to a decrease in double bond character of the C═O bond (and an increase in charge on oxygen) in acetanilides because the C═O bond is two bonds removed from the aromatic system (Chart 1).[3] A possible reason for the shielding of ^{17}O in aromatic isocyanates upon alkyl substitution in ortho position (and assumed twisting), on the other hand, was less obvious, and attractive van der Waals interactions with the substituent were tentatively suggested.[2]

CHART 1: Resonance Structures in Benzaldehydes and Acetanilides[3] That Explain the ^{17}O (De)Shielding Observed upon Twisting

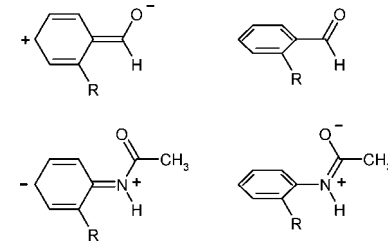

It follows from the above that the prediction of whether ^{17}O in terminal oxygen systems is shielded or deshielded upon torsion is not necessarily straightforward. Fortunately, the ^{17}O NMR spectra of substituted *N*-sulfinylanilines are also available, and in analogy to aldehydes and nitro compounds (and the

† To whom correspondence should be addressed. E-mail: muchall@alcor.concordia.ca. Phone: (514) 848-2424, extension 3342. Fax: (514) 848-2868.

10.1021/jp804670h CCC: $40.75
Published on Web 08/28/2008

majority of similar functional groups),[1] they also show a deshielding upon introduction of increasing bulk in ortho position.[8]

Unfortunately, though, in all cases mentioned above, twisting is invoked through steric hindrance, and while it is assumed that alkyl groups on an aromatic ring do not have a large electronic effect on the ^{17}O nuclear shielding in the functional group, that assumption might be incorrect. For example, it struck us as odd that the 2,6-dimethylphenyl isocyanate should be twisted,[2] there being no contacts between the NCO atoms and hydrogen atoms of the substituents. In addition, from our experimental ^{17}O NMR studies, we were interested in the chemical shift change upon twisting of the unsubstituted *N*-sulfinylaniline. The calculation of chemical shifts (or isotropic shieldings) is nowadays straightforward, and computational chemistry, fortunately, does not encounter certain experimental problems. Computationally, twisting can easily be studied free of perturbing substituents by simply freezing torsion angles.

Finally, computational chemistry can also provide insight into the origin of isotropic shieldings[9−12] and their changes upon twisting and substitution because the isotropic shielding can be partitioned into its orbital contributions. Dahn has provided a very readable excerpt on the topic.[13] Particularly useful in π-systems is the fact that the (mostly deshielding) paramagnetic component of the isotropic shielding is inversely proportional to the excitation energy (or difference in orbital energies) of the molecule,[14] as expressed in the Karplus−Pople equation.[15] Thus, the important $n_O \rightarrow \pi^*_{C=O}$ interaction in carbonyl compounds that gives rise to a low-energy electronic absorption signal is also largely responsible for the deshielding of the ^{17}O nucleus in a magnetic field, if the mixing of the orbitals is associated with an angular momentum.

In this paper, we first present the calculated oxygen shieldings in the substituted systems (benzaldehydes, nitrobenzenes, phenyl isocyanates, acetanilides, and *N*-sulfinylamines, Chart 2) to provide an assessment of how well the chosen model chemistry performs against experiment. The results are compared to the calculated response of the oxygen shielding in relaxed torsional scans for benzaldehyde (Ph−CHO, **1**), nitrobenzene (Ph−NO_2, **2**), phenyl isocyanate (Ph−NCO, **3**), acetanilide (Ph−NHCO-CH_3, **4**), and *N*-sulfinylaniline (Ph−NSO, **5**). Charges and orbital contributions to the isotropic shieldings are presented in both the substitution and the torsion studies to gain insight into the source of the observed changes. We will show that only a detailed computational study of each molecular system of interest allows a conclusion on the change in shielding, its direction, and its origin.

2. Computational Details

All calculations were carried out using Gaussian 03.[16] Full or partial geometry optimizations were performed with the Becke3[17]−Lee, Young, and Parr[18] hybrid density functional (B3LYP)[19] and the 6-31+G(2d,2p) basis set. Where a discrepancy between previously reported and calculated torsion angles was encountered (2,6-dimethylbenzaldehyde and acetanilide), geometries were checked against those from MP2/6-31+G(2d,2p) as well as from B3LYP/6-31+G(2d,2p) in acetonitrile with the COSMO polarizable continuum solvent model;[20−22] differences to B3LYP/6-31+G(2d,2p) results in the gas-phase were not found. Frequency calculations for the fully optimized structures returned real frequencies only. Total energies and zero-point vibrational energy corrections are reported in Table 1. The partial optimizations refer to relaxed scans, and only the torsion angle of interest was frozen. Shielding tensors were obtained with the OPBE functional (Cohen and Handy's OPTX[23] combined with the Perdew−Burke−Ernzerhof PBE[24] functional) and the 6-311++G(2df,pd) basis set, as OPBE has been shown to give a superior performance for magnetic shieldings and chemical

CHART 2: Representation of the Geometry-Optimized Molecular Species 1-5 and Their Methyl (Me) and *tert*-Butyl (Bu) Substituted Derivatives[a]

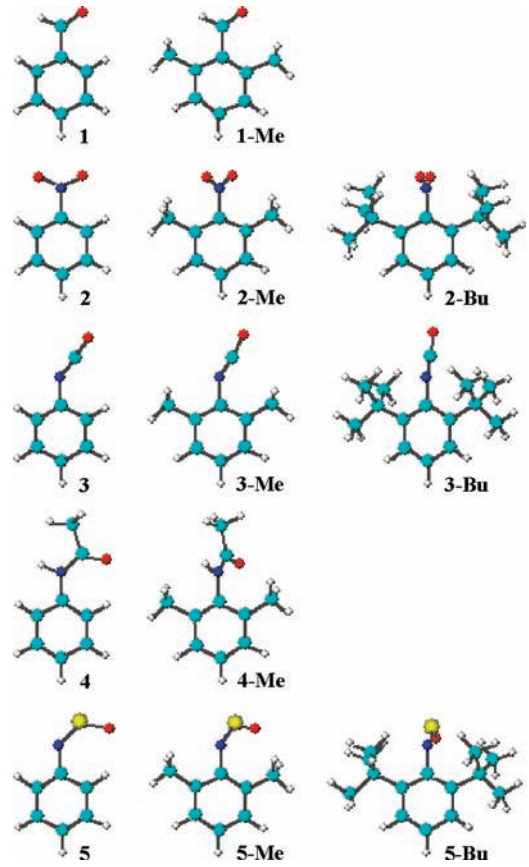

[a] Color code: C, light blue; H, white; N, dark blue; O, red; S, yellow.

TABLE 1: Total energy[a] [E_{tot}, au] and Zero-Point Vibrational Energy Correction[a] [ZPVE, au], Torsion Angle[a] [φ, deg], Charge on Oxygen [q, au], Oxygen Isotropic Shielding[b] [σ_{iso}, ppm], and Experimental ^{17}O Chemical Shift [δ, ppm] for Aromatic Aldehydes, Nitro Compounds, Isocyanates, Acetanilides, and *N*-Sulfinylanilines

	E_{tot}	ZPVE	φ	q	σ_{iso}	δ
1	−345.608 151	0.109 611	0	−0.539	−282	564[c,d]
1-Me	−424.244 753	0.164 956	0	−0.550	−316	585[c,d,e]
2	−436.793 347	0.103 031	0	−0.378	−260	575[d,f]
2-Me	−515.430 220	0.158 052	56	−0.365	−319	629[d,f]
2-Bu	−751.309 819	0.327 673	76	−0.362	−348	657[d,f,g]
3	−399.769 703	0.103 642	0	−0.498	163	111[d,h]
3-Me	−478.413 434	0.158 699	0	−0.511	177	101[d,h]
3-Bu	−714.295 492	0.327 758	90	−0.527	186	99[d,h,i]
	−714.295 484	0.327 894	0	−0.530	184	
4	−440.312 265	0.154 873	0	−0.621	−82	355[d,j]
4-Me	−518.950 627	0.209 704	65	−0.623	−70	343[d,j]
5	−759.811 607	0.099 732	0	−0.891	−176	406[k,l]
5-Me	−838.449 922	0.154 648	50	−0.885	−183	418[k,l]
5-Bu	−1074.325 115	0.323 517	92	−0.868	−205	427[k,l,g]

[a] From B3LYP/6-31+G(2d,2p). [b] From OPBE/6-311++G(2df,pd). [c] From ref 4. [d] In acetonitrile at 75 °C, referenced to external water. [e] For the 2,4,6-trimethyl species. [f] From ref 5. [g] For the 2,4,6-tri-*tert*-butyl species. [h] From ref 2. [i] For the 2,6-diisopropyl species. [j] From ref 3. [k] From ref 8. [l] In chloroform, referenced to external water.

shifts compared to other popular density functional methods.[25] We employed the gauge including atomic orbitals (GIAO) method[26−28] and report the isotropic shieldings σ_{iso} as opposed to chemical shifts δ, mainly to avoid the issues associated with determining a water-reference shielding.[29] Note that because δ and σ_{iso} are related through σ_{iso}^{ref} of the reference as $\delta = \sigma_{iso}^{ref} - \sigma_{iso}$, "deshielding" for δ indicates larger positive numbers while σ_{iso} values decrease and usually become more negative. To uncover the orbital contributions to the isotropic shieldings, we performed natural chemical shielding (NCS) analyses.[30] These and charges were determined with the natural bond orbital (NBO) method[31] as implemented in Gaussian 03. Selected wave functions, from B3LYP/6-31+G(2d,2p), were obtained, and topological analyses of the electron densities were carried out within the framework of the quantum theory of atoms in molecules (QTAIM),[32] using the program AIM2000.[33] Molecular orbitals were obtained from B3LYP/6-31+G(2d,2p) and plotted from Molekel.[34,35]

3. Results and Discussion

Substituted Aromatic Systems. The molecules studied are shown in Chart 2. Only the lowest energy conformer or configuration was considered. Substituted derivatives are designated only with respect to the type of substituent; thus, 2,6-dimethylbenzaldehyde is given as **1-Me**. Obviously, compounds such as benzaldehyde and nitrobenzene have received great attention in the past, and therefore, the available literature (e.g., on their geometry) is vast. Here, we are focusing entirely on the torsion angle; other references are not included. In the following, the functional groups are discussed separately with respect to geometries, shieldings, and orbital contributions to the shieldings.

Aldehydes. ***Geometry.*** The torsion angles are reported in Table 1. The unsubstituted Ph−CHO (**1**) is planar, in accord with gas-phase electron diffraction[36] and early microwave[37] results and even with X-ray data in cocrystals, where **1** is found to be mostly planar with packing-induced twists of less than 5°.[38] In contrast to this consensus, 2,6-dimethyl Ph−CHO (**1-Me**) is also calculated to possess a planar global minimum, whereas experimental torsion angles differ. Thus, **1-Me** is reported twisted by 28°, as determined from the absorption intensity of its K-band in a UV spectroscopic study,[39] the closely related 2,4,6-trimethylbenzaldehyde was deduced to have a 33° twist by ^{17}O NMR spectroscopy,[4] yet the latter was determined to be planar by molecular mechanics calculations[4] and also shows a twist of only about 7° in a cocrystal (X-ray data)[40] and could thus be considered planar. We therefore validated our result for **1-Me** against the minimum geometries obtained from calculations using MP2 and B3LYP in solvent (acetonitrile, COSMO solvent field), but both approaches also returned planar **1-Me**. With respect to **1**, **1-Me** exhibits a shorter C−C (148.0 pm in **1**, 147.9 pm in **1-Me**) and a longer C═O (121.3 pm in **1**, 121.7 pm in **1-Me**) bond, neither of which support the notion of decreased delocalization[7] or increased double bond character of C═O. Finally and in line with the above, the calculated NBO charge on oxygen in **1-Me** is more negative than that in **1** (Table 1).

Shielding. The isotropic shieldings σ_{iso} for oxygen in **1** and **1-Me** are given in Table 1 together with the available experimental chemical shifts δ. Because our aim is to reproduce small differences in δ upon substitution, the chemical shifts listed in Table 1 are taken from an investigation of a series of similar compounds; reported values for ^{17}O in **1** of 562 (in dioxane) and 568 (neat) ppm[41] at 303 K or 562 (in acetonitrile) and 574 (in CCl_4) ppm[42] at 40 °C are not included in Table 1 because data for **1-Me** were not available from the same study. The experimentally found downfield shift of 21 ppm in **1-Me**, which is based on δ for 2,4,6-trimethylbenzaldehyde,[4] with respect to **1** is reproduced well, with a calculated deshielding of 34 ppm (σ_{iso}(**1**) − σ_{iso}(**1-Me**)). The shift of 21 ppm had been attributed to a twist of 33° upon ortho substitution, based on a δ–torsion angle relationship for aryl ketones.[4] Yet from the data in Table 1, it follows that the correct deshielding is calculated even in the absence of a twist between aromatic and CHO moieties, which illustrates the electronic effect of the methyl group and the fact that it should not be neglected.

TABLE 2: Important Orbital Contributions [ppm] to the Oxygen Isotropic Shielding in Aromatic Aldehydes, Nitro Compounds, and *N*-Sulfinylanilines[a]

	1	**1-Me**	**2**	**2-Me**	**2-Bu**	**5**	**5-Me**	**5-Bu**
σ_{X-O}	−156	−122	−185	−6[b]	−136[b]	−237	−234	−267
$\pi_{X=O}$	(18)[c]	(36)[c]	72[d]	161[b,d]	−67[b,d]	36[e]	26[e]	68[e]
n_O-σ	−100	−83	118	−129	53	−71	−9	25
n_O-π	−303	−374	−493	−609[b]	−464[b]	−149	−182	−238
σ_{OC-H}	−8	−28						
$\pi_{C=C}$			−38[b]	−8[b]	−5[b]	20	−1	−6
n_S						−20	−24	−19
n_N						−21	−40	−40
total	−567	−607	−526	−591	−619	−442	−464	−471

[a] From OPBE/6-311++G(2df,pd). [b] Averaged value for the two oxygen atoms. [c] Not included in the total. [d] Summed from a π_{NO2} (17% N, 71% O1, 12% O2, calculated as an n_O-π; the "true" n_O-π has 94% oxygen character) and a $\pi_{N=O}$ with 41% N, 59% O character. [e] This orbital is described as n_O-π with 79% oxygen character, while the "true" n_O-π has 92% oxygen character.

Orbital Contribution. Table 2 gives the important orbital contributions to σ_{iso} of oxygen in **1** and **1-Me**. Initially, contributions were considered important if they were larger than 10 ppm, and deshielding contributions only are listed. Smaller values and shielding contributions were considered where needed for the interpretation. As found before for oxygen in formaldehyde,[30] the largest deshielding contribution stems from the π-type electron lone pair on oxygen, n_O-π. The difference in the total sums for **1** and **1-Me** from Table 2, −40 ppm, corresponds well to the calculated deshielding of −34 ppm from Table 1, and the observed effect is therefore captured by the deshielding contributions alone, if somewhat overestimated. There are numerous small changes for other orbital contributions to σ_{iso} between **1** and **1-Me**, the largest being for $\pi_{C=O}$ (listed in parentheses), which is not included in the total because it does not change the above conclusion. While all orbital contributions listed in Table 1 change upon substitution, it is clear that the main reason for the observed deshielding of ^{17}O in **1-Me** (calculated as well as experimental) lies in the increased contribution from n_O-π. This, in turn, is a consequence of the smaller energy gap between the mixing orbitals, HOMO (n_O-π) and LUMO ($\pi^*_{C=O}$), in **1-Me**. Because of methyl substitution, the HOMO in **1-Me** is destabilized, which decreases the gap from 5.15 eV in **1** to 4.92 eV in **1-Me**, resulting in a stronger $n_O-\pi$ contribution to the deshielding. The trend does not change if the calculated electron affinity (EA) is used instead of the (questionable) LUMO energy,[43] and it even becomes more pronounced because the EA is calculated to be the same for **1** and **1-Me** (0.22 eV), but the HOMO in **1-Me** is destabilized by about 0.3 eV.

Nitro Compounds. ***Geometry.*** The unsubstituted Ph−NO_2 (**2**) is planar (Table 1), as was found in a microwave[44] and the latest electron diffraction study,[45] even though earlier electron

diffraction studies had reported nonplanar minimum geometries.[46,47] Nitrobenzene (**2**) is also reported planar in the crystal from X-ray diffraction studies, with a twist of less than 4°,[48,49] and from earlier HF calculations.[46] The calculated torsion angle for 2,6-dimethyl Ph−NO_2 (**2-Me**) of 56° agrees well with the 66° found for the related 2,4,6-trimethylnitrobenzene in the crystal structure.[50] Not surprisingly, we find 2,6-di-*tert*-butyl Ph−NO_2 (**2-Bu**) to be twisted even more, but the torsion angle does not reach 90°. For the nitro series, the calculated changes in bond length are in accord with the suggested decrease in delocalization and increase in double bond character,[1,2,5] as the C−N distance increases from 147.3 (**2**) to 147.5 (**2-Me**) to 148.2 (**2-Bu**) pm and the N═O distance decreases from 122.6 (**2**) to 122.5 (**2-Me**) to 122.4 (**2-Bu**) pm. In accord with this, as had been suggested,[1] there is a loss in negative charge on oxygen (Table 1), a trend opposite to that found in the aldehyde series above.

Shielding. The oxygen isotropic shieldings and available chemical shifts for **2**, **2-Me**, and **2-Bu** are given in Table 1. The consecutive downfield shifts in δ upon substitution are reproduced well by the calculations. For an experimental deshielding of 54 ppm from **2** to **2-Me**, we calculate a deshielding of 59 ppm, and the overall shift of 82 ppm is calculated to be 88 ppm. The 2,4,6-tri-*tert*-butylnitrobenzene used in the experiment[5] is therefore adequately represented in the calculations by **2-Bu**. A δ–torsion angle (determined by X-ray diffraction) relationship was established from seven compounds, among those **2** and 2,4,6-trimethylnitrobenzene, but the large ^{17}O chemical shift of 2,4,6-tri-*tert*-butylnitrobenzene (657 ppm) was unexpected and did not fit the δ–torsion angle relationship[5] because the 90° cutoff was already reached by 9-nitroanthracene with a torsion angle of 85° and a δ of only 637 ppm.[1] A data point corresponding to 657 ppm was impossible to accommodate, and possible reasons given included alteration of the solvent structure around the nitro group by the *tert*-butyl substituents and distortion of the benzene ring from planarity as a result of steric crowding.[1] The latter can be discarded because we calculate a maximum deviation of 2° from planarity for any atoms lying in the aromatic plane. And the former can also be excluded because the correct downfield shift for **2-Bu** is calculated already in the gas phase. In light of our results discussed above, namely, that **1-Me** already shows a downfield shift without an accompanying twist, it seems much more reasonable that a simple, linear δ–torsion angle relationship as was suggested[1,5] does not exist but that electronic effects simply cannot be neglected.

Orbital Contribution. The important orbital contributions to σ_{iso} are given in Table 2. Even though there are C−H···O interactions in **2-Bu** with methyl hydrogen atoms (one each for each oxygen atom; see Chart 3), there is no significant (−0.4 ppm) σ_{C-H} contribution to σ_{iso}; the C−H···N interactions contribute somewhat more (−4.5 ppm). In contrast to the discussion for the aldehydes above, the total orbital contributions calculated from the deshielding values alone are not a good representation of the observed deshielding within the series, as the smallest such total is summed for **2-Bu**. It is obvious that the total for these orbital contributions has to be "corrected" by shielding contributions, which has been done for the totals given in Table 2. The differences in these totals of −65 and −93 ppm for **2-Me** and **2-Bu**, respectively, from that of **2** agree well with the calculated changes in σ_{iso} of −59 and −88 ppm, respectively, which is an indication that all important orbital contributions have been considered. Unfortunately, an inspection of the change in a specific orbital contribution for the nitro series shows that any interpretation as to the source is probably hopeless. The only straightforward change is observed for the $\pi_{C=C}$ contribution, and it is as expected.

CHART 3: Network of Bonding Interactions in 2-Bu, 3-Bu (Twisted), 4, 4-Me, 5, 5-Me, and 5-Bu[a]

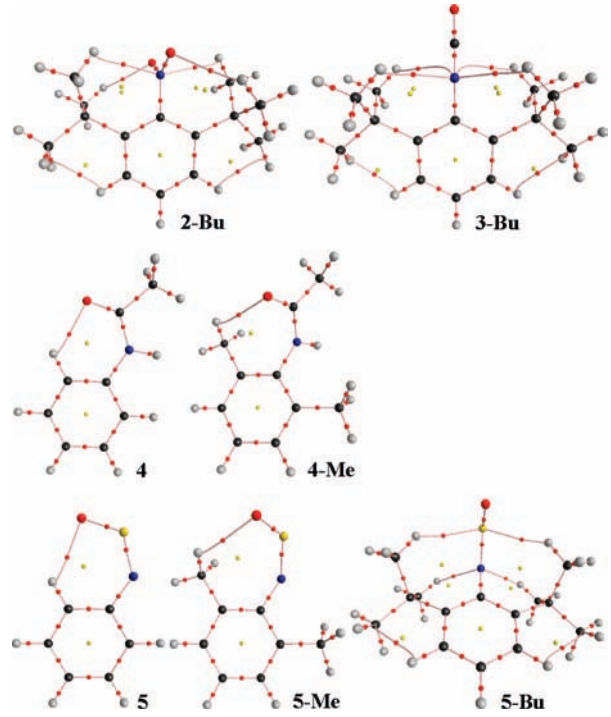

[a] The small red spheres and their associated lines identify bonding interactions between atoms. Color code of the large spheres: C, black; H, white; N, blue; O, red; S, yellow.

Isocyanates. ***Geometry.*** Data on the geometries of aromatic isocyanates are scarce, but in accord with a microwave study,[51] Ph−NCO (**3**) is calculated to be planar (Table 1). In fact, so are 2,6-dimethyl Ph−NCO (**3-Me**) and even 2,6-di-*tert*-butyl Ph−NCO (**3-Bu**) (conformer not shown in Chart 2). For **3-Bu**, though, there is also a perpendicular conformer of about equal energy (Table 1 and Chart 2). Similar to the change in charge in the aldehyde series, the negative charge on oxygen increases in the isocyanate series (Table 1).

Shielding. The oxygen isotropic shieldings for **3**, **3-Me**, and **3-Bu** (both planar and twisted) are given in Table 1 together with the available experimental chemical shifts. In contrast to ^{17}O in the aldehydes and nitro compounds discussed above, in the isocyanates it is shielded upon ortho substitution of the aromatic ring. The experimental upfield shift from **3** to **3-Me** is 10 ppm,[2] compared to 14 ppm calculated. The overall shielding of 12 ppm for ^{17}O in **3** to that in 2,6-diisopropylphenyl isocyanate is in reasonable agreement with the calculated value of 21 ppm, if the planar **3-Bu** is considered. It is a reasonable assumption that 2,6-diisopropylphenyl isocyanate with its smaller isopropyl groups is planar, but in any case the shielding to the twisted **3-Bu** is close with 23 ppm. Just as in the aromatic aldehydes above, the 21 ppm shielding in the planar series is thus achieved through substitution alone, not through a twist, and especially the difference in σ_{iso} for **3-Me** and **3-Bu** shows that it is not necessarily reasonable to assume that the electronic effect of methyl and *tert*-butyl groups on the isotropic shielding of the oxygen nucleus is comparable in these aromatic systems.

The observed shielding upon substitution was tentatively explained through "attractive van der Waals interactions between the proximate groups".[2] This can be ruled out, though, because

TABLE 3: Important Orbital Contributions [ppm] to the Oxygen Isotropic Shielding in Aromatic Isocyanates and Anilides[a]

			3-Bu			
	3	**3-Me**	twisted	planar	**4**	**4-Me**
σ_{C-O}	−51	−79	8	−2	−38	−45
$\pi_{C=O}$	−12[b]	40[b]	28[b]	30[b]	−12	−72
σ_{N-C}[c]	−14	−9	−16	−14		
n_O-σ	−85	−79	−112	−111	−106	−126
n_O-π					−190	−108
σ_{C-C}[d]					−17	−16
σ_{C-H}[e]					−10	−10
n_N					1	30
total	−162	−127	−92	−97	−372	−347

[a] From OPBE/6-311++G(2df,pd). [b] This orbital is $\pi_{C=O}$-type for **3** with 73% oxygen character; it is described as n_O-π for **3-Me** (78% on oxygen) and for the twisted **3-Bu** (80%), where the "true" n_O-π has 81% and 82% oxygen character, respectively. The two n_O-π orbitals have the same contribution and oxygen character in the planar **3-Bu**. [c] For N═C. [d] From the carbonyl group, OC−CH_3. [e] From a methyl C−H bond.

topological analyses of the electron densities of both the planar and the twisted **3-Bu** only reveal bonding interactions between hydrogen atoms on the methyl groups and the nitrogen atom of the NCO group (C−H···N, Chart 3). It is not easy to see how these weak interactions two bonds from the NCO oxygen atom should influence its isotropic shielding to such a large amount. In addition, the shielding is already observed with the much smaller methyl groups, which do not show any interactions with the NCO moiety.

Orbital Contribution. It was noted early that the ^{17}O signal of isocyanates appears at a much higher field than those of other terminal oxygen systems, and this was attributed to a greater single bond character of the C═O bond.[2] The small δ is now better understood in terms of the ^{17}O shielding tensor in that the tensor component along the linear NCO array ($\sigma_{||}$) is not deshielding, and isocyanates in this respect behave like linear molecules.[52] It is a consequence of the magnetically inactive mixing of n_O-π and $\pi^*_{C=O}$, even though the two π^* orbitals with oxygen coefficients are not strictly degenerate. In accord with this, the calculated orbital contribution for n_O-π is shielding and therefore missing from Table 3. As a consequence, the total summed deshielding contributions are less than those for aldehydes and nitro compounds (Table 2). The overall shielding (in σ_{iso} and δ) found in the isocyanate series upon substitution is reproduced well from the deshielding orbital contributions only when $\pi_{C=O}$ is included, which switches from deshielding in **3** to shielding in **3-Me** and **3-Bu**. The shielding effect is overestimated from the totals in Table 3, which suggests again that other orbital contributions should not be neglected.

Again, and similar to the nitro series, the reason for the overall shielding is not as obvious as in the benzaldehyde series, as the changes to σ_{iso} are not monotonic across the three isocyanates for a specific orbital contribution. As a final note, the weak C−H···N interactions in **3-Bu**, as expected, do not contribute to σ_{iso} of the oxygen atom; only one such contribution with a value of −0.3 ppm is found in the twisted **3-Bu**.

Acetanilides. ***Geometry.*** While acetanilide (Ph−$NHCOCH_3$, **4**) is found to be twisted up to 20° in the crystal by X-ray [6,53] and neutron diffraction,[54] it is determined to be planar in the gas-phase from electronic[55] and microwave[56] spectra. In accord with the experimental gas-phase structures and in contrast to an early molecular mechanics calculation,[3] **4** has been calculated to be planar using B3LYP and MP2 with the 6-31G(d) basis set[56] and CASSCF/cc-pVDZ[57] (even though the higher-energy rotamer for the methyl group was identified as the global minimum) and with B3LYP/6-31G(d,p).[58] The finding of a planar minimum structure for **4** does not change with the larger basis set employed here (Table 1) or with MP2/6-31+G(2d,2p) and B3LYP in solvent (acetonitrile, COSMO solvent field). For **4-Me**, we calculate a twist of 65° (Table 1), in good agreement with the torsion angles of 63° from X-ray diffraction[59] and 58° from molecular mechanics calculations.[3] In contrast to the suggested increased importance of the resonance structure that does not involve the ring (Chart 1) upon twisting,[3] we do not calculate a lengthening of the C═O bond for **4-Me**. In support of this structure, we calculate a slight increase in negative charge (Table 1), even though the change is minimal compared to that found for the aldehydes, nitro compounds, and isocyanates above.

Shielding. The isotropic shieldings and chemical shifts for oxygen in **4** and **4-Me** are given in Table 1. There is a perfect agreement between experimental and calculated shielding effects (12 ppm) upon substitution. The size of the shielding effect is comparable to that found in the aromatic isocyanates, but while it occurs between the planar **3** and **3-Me**, in **4** and **4-Me** it is accompanied by a twist.

Orbital Contribution. The important orbital contributions to σ_{iso} of **4** and **4-Me** are given in Table 3. There is no significant contribution (−1.6 ppm) from the ortho C−H bond that has been suggested to be involved in an intramolecular C−H···O interaction,[54] even though a topological analysis of the electron density confirms this weak interaction (Chart 3, density is 0.119 e/Å^3). Similarly, the contribution from the methyl C−H bond involved in a weak interaction in **4-Me** (Chart 3) is small (−0.7 ppm).

The sum of the deshielding contributions (Table 3) fails to capture the observed shielding effect on going from **4** to **4-Me**, but the overall shielding can be reproduced with the inclusion of the n_N contribution, which becomes much more shielding for the oxygen nucleus in **4-Me** (Table 3). Upon twisting (by 65°), the interaction of the nitrogen lone pair with the π-system of the aromatic ring is lost to a large degree, and n_N becomes more available for the amide resonance. This agrees with the smaller δ for ^{17}O found in nonconjugated, aliphatic amides.[3] The increased shielding of oxygen from n_N is accompanied by a particularly large increase in shielding from n_O-π. This orbital contribution is the main reason for the observed shielding (calculated and experimental) of ^{17}O in **4-Me**, and it should again be a consequence of the change in energies of the molecular orbitals involved. This is confirmed from the raw orbital energies. In **4**, the HOMO−2 (n_O-π)/LUMO ($\pi^*_{C=O}$) gap is 6.48 eV, which increases to 6.57 eV in **4-Me** mainly because of the destabilization of the LUMO in **4-Me**. On the other hand, the calculated electron affinities for **4** and **4-Me** are almost identical (−0.75 and −0.76 eV, respectively), which leads to a slightly smaller energy gap in **4-Me** because HOMO−2 is less stable by 0.1 eV than in **4**.

N*-Sulfinylanilines.** ***Geometry. In accord with UV,[60] NMR,[61] microwave,[62] and X-ray diffraction[63] data, as well as with previous calculations using HF, B3LYP, B3PW91, and MP2 methods with various basis sets,[63−65] Ph−NSO (**5**) is calculated to be planar (Table 1). There is an increasing twist with methyl and *tert*-butyl substitution, and the calculated torsion angles are in accord with those determined from crystal structures for 2,6-diethyl-*N*-sulfinylaniline (55°)[63] and 2,4,6-tri-*tert*-butyl-*N*-sulfinylaniline (92°),[66] respectively. The change in charge on oxygen

CHART 4: Selected Molecular Orbitals of *N*-Sulfinylanilines

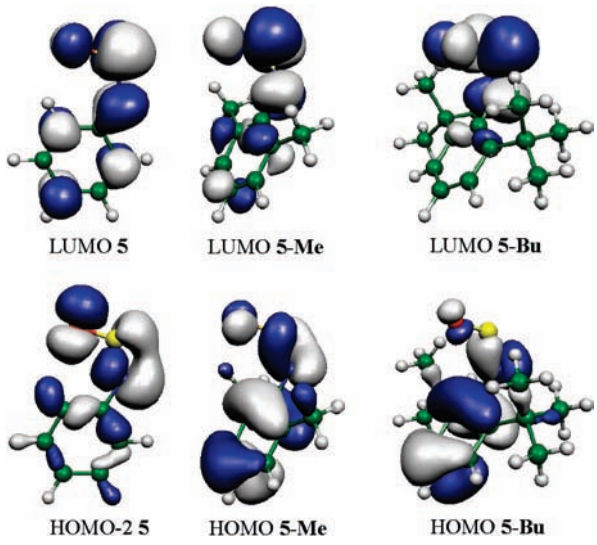

is similar to that found in the nitro series in that there is a loss of negative charge.

Shielding. The oxygen isotropic shieldings and available chemical shifts for **5**, **5-Me**, and **5-Bu** are given in Table 1. Again, values reported for incomplete series, such as 417 ppm for **5** in CCl_4 at 35 °C with dioxane as external reference,[67] were ignored, and the calculated σ_{iso} values certainly support this decision. Similar to the change upon methyl substitution in the aldehyde and nitro series, there is a downfield shift of the oxygen signal, but the change from **5** to **5-Me** is smaller (Table 1). The overall change in σ_{iso} of 29 ppm agrees well with the change in δ of 21 ppm, suggesting that **5-Bu** is a proper model for 2,4,6-tri-*tert*-butyl-*N*-sulfinylaniline, which was used in the experimental work.[8]

Orbital Contribution. The important orbital contributions to σ_{iso} are given in Table 2. Chart 3 shows that all three *N*-sulfinylanilines exhibit weak interactions from C−H bonds to atoms of the NSO group; that in **5** has been reported before.[65] For **5-Bu**, these are in accord with two short intramolecular C−H···S distances in 2,4,6-tri-*tert*-butyl-*N*-sulfinylaniline reported from a crystal structure analysis.[66] For all three compounds, these C−H bonds contribute only small deshielding amounts to σ_{iso} (−1.7 ppm in **5**, −2.1 ppm in **5-Me**, −2.8 ppm each in **5-Bu**). In contrast to aromatic aldehydes, nitro compounds, and even **4**, where the n_O-π contribution dominates σ_{iso}, for the *N*-sulfinylanilines it is the σ_{S-O} contribution.

To reproduce the deshielding trend observed in σ_{iso} and δ, the shielding from $\pi_{S=O}$ and the varying contribution from $\pi_{C=C}$ have to be considered (Table 2). The largest change in orbital contribution upon substitution is calculated for n_O-π, as was found above for the aromatic aldehydes, and this is the main reason for the observed deshielding in **5-Me** and **5-Bu**. In **5**, n_O-π is HOMO−2; higher-lying occupied orbitals do not have such a coefficient on oxygen. And while in **5-Bu** n_O-π is HOMO−3, the HOMO has a coefficient on oxygen that resembles that in n_O−π. The energy gap for an "n_O-π"/$\pi^*_{C=O}$ mixing therefore decreases from 5.10 eV in **5** to 3.56 eV in **5-Bu**. For **5-Me**, σ/π-separation for the orbitals is lost because of the 50° twist, and the distorted "π-type" HOMO has enough σ-character on oxygen to allow for a magnetically active mixing with the LUMO, as can be seen from the slightly different orientations of the coefficients on oxygen in HOMO and LUMO.

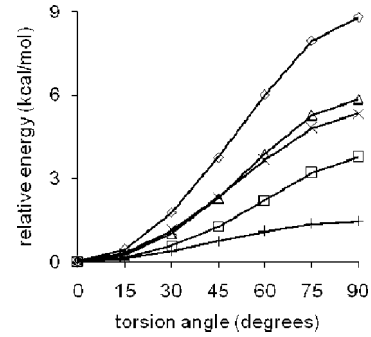

Figure 1. Relative energy as a function of the torsion angle: (◇) Ph−CHO (**1**); (△) Ph−NO_2 (**2**); (+) Ph−NCO (**3**); (□) Ph−$NHCOCH_3$ (**4**); (×) Ph−NSO (**5**).

The relevant "n_O-π" orbitals discussed here are depicted in Chart 4 along with the respective LUMO.

Relaxed Torsional Scans. While the experimentally observed changes in δ upon substitution can be reproduced well computationally, it is possible to distill two main points for further consideration from the above. First, the observed changes in δ are not always due to conformational changes. And second, it is not always possible to determine which orbital contribution causes the observed shielding or deshielding. Presumably, this last fact is due to the perturbing introduction of substituents. We therefore performed relaxed torsional scans for the parent compounds and determined the changes in σ_{iso} and charge of oxygen as well as the change in σ of the orbital contributions, which are discussed separately below.

The energy profiles for rotation of the substituent against the phenyl ring in **1**−**5** are given in Figure 1. The energies obtained for the 90° species are identical to those obtained for the transition states for the torsions. They agree reasonably well with the upper values for experimental barriers to torsion for **1** (summarized in ref 68) and **2** (summarized in ref 69) and with values given for **3**[70] and **5**.[62] A closer comparison with experiment will not be drawn here, as experimental ranges for the barriers are typically large for these compounds, strongly depend on the method and phase used and because this is not the focus of the present paper. Similarly, it is not the aim of this paper to summarize the work that has been performed computationally on torsional barriers and their origins either (see, for example, the recent work on **2**).[69]

Change in Isotropic Shielding and Charge on Oxygen. Figure 2 shows the torsional dependence of the isotropic shielding of oxygen in **1**−**5**, with some expected and some surprising outcomes. For Ph−CHO (**1**) and Ph−NO_2 (**2**) (parts a and b of Figure 2), the experimentally observed deshielding with substitution is also found upon torsion, and this is also true for the shielding observed in Ph−NCO (**3**) and in Ph−$NHCOCH_3$ (**4**) (parts c and d of Figure 2). In other words, in the benzaldehyde system, the deshielding found upon substitution of **1**, i.e., for the planar **1-Me**, is also achieved upon a twist of **1**, but in **1-Me** it is not the result of a twist. The same holds for the shielding in the phenyl isocyanate system (the **3** series). For **4**, σ_{iso} does not change beyond 60°. This is not a problem associated with the amide functionality, though, because there is a monotonic change in σ_{iso} from −107 to −73 ppm for the higher-energy syn conformer of **4** (with an HNCO dihedral of 0°; plot not shown).

The unusual trend in **4** is in fact enhanced in **5** (Figure 2e) in that shielding is observed only up to 45°, with a similar amount of deshielding up to 90°. The consequence is a torsional profile for **5** with four shielding maxima through 360°, while **1**−**4** only

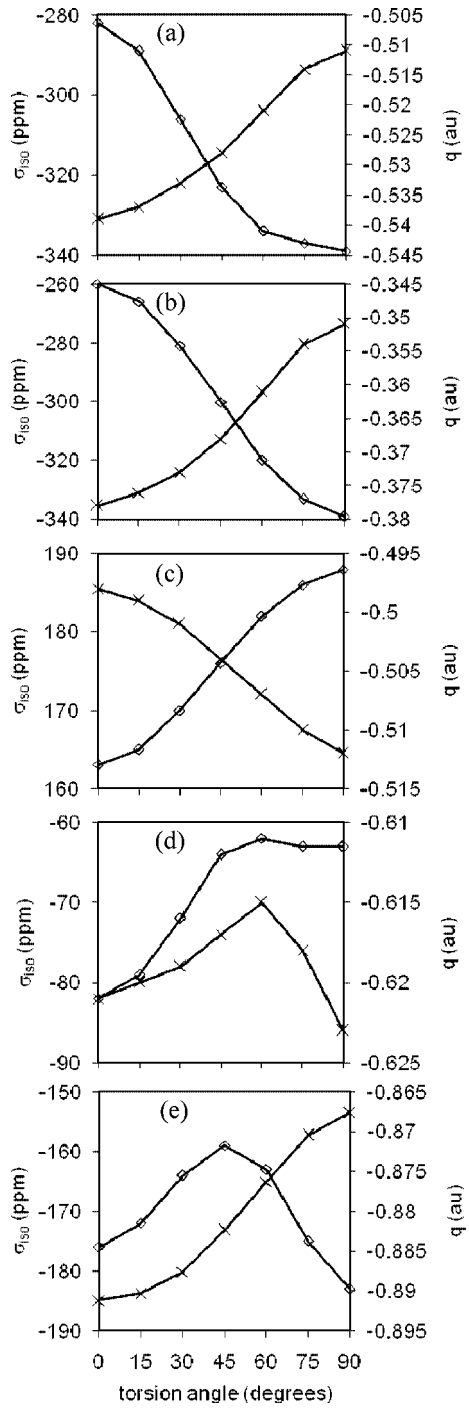

Figure 2. Isotropic shielding (σ_{iso}, ◇) and charge (q, ×) of oxygen as a function of the torsion angle: (a) Ph−CHO (**1**), (b) Ph−NO_2 (**2**), (c) Ph−NCO (**3**), (d) Ph−$NHCOCH_3$ (**4**), and (e) Ph−NSO (**5**).

possess two maxima in σ_{iso}. This behavior for **5** is not found upon substitution, again demonstrating the electronic effect of the methyl and *tert*-butyl substituents.

The dependence of the NBO charge on the torsion angle is given in Figure 2 with the secondary axis; the trends for charges in **1**, **2**, **3**, and **5** upon twisting obtained with QTAIM (not shown) are identical, but changes are smaller. For **4**, where the change in NBO charge is already small (Figure 2d), the negative QTAIM charge increases monotonically, but in either case the changes in charge are so small that a discussion of the differences might not be meaningful. Only for Ph−NO_2 (**2**), Ph−NCO (**3**), and Ph−NSO (**5**) does the change in charge on oxygen upon torsion agree with the trend upon substitution.

CHART 5: Resonance Structures in Ph−NCO (3) and Ph−NSO (5) That Explain the Gain and Loss, Respectively, in Negative Charge of Oxygen upon Twisting

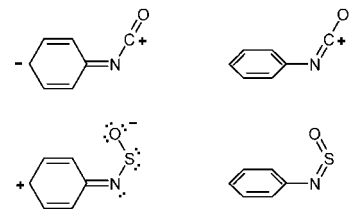

Upon torsion, the negative charge decreases in **1**, **2**, **4** (up to 60°), and **5**; it increases in **3**. For the unsubstituted **1**, **2**, and **4**, the direction of the change is thus as anticipated from resonance arguments as given in Chart 1 and in the literature.[1,3] That the change in **5** is similar in kind suggests a planar resonance structure that also involves the aromatic ring (Chart 5). Finally, such a resonance structure can also explain the negative charge increase found upon twisting of **3** (Chart 5).

As is evident from Figure 2, all changes in charge between planar and perpendicular species are small, as was found for the change upon substitution, and for **2**, it has been concluded that a conformational change from planar to perpendicular does not lead to a change in (Mulliken) charge.[46] But while small, these changes are important, as seems to be suggested in Figure 2 from their relation with the isotropic shielding of oxygen, a sensitive probe.

Change in Orbital Contribution to the Isotropic Shielding of Oxygen. It is obvious from Figure 2e that the relationship between σ_{iso} and the charge upon torsion breaks down in **5**; it already did not hold for substitution in **1** and **4**. Rather, as can be expected from the data in Tables 2 and 3 and their discussion, orbital interactions should be considered, as the important molecular orbitals are easily perturbed by changes in molecular structure, and torsion can be such a change.

The changes in the orbital contributions to σ_{iso} upon torsion of **1**−**5** are shown in Figure 3. For **1** (Figure 3a), the major change in the region 0−75° lies in the n_O-π contribution (×), which was also identified as the orbital responsible for the deshielding upon substitution. The dependence of the orbital energies of the three highest occupied orbitals is given in Figure 4a. It is interesting that the HOMO (n_O-π) energy is essentially constant during the twist, but HOMO−2, which is π-type in the planar **1** and becomes an additional n_O-π (bonding interactions with coefficients on the ring; the HOMO n_O-π shows antibonding interactions) during the twist, is destabilized, thus giving rise to the observed deshielding. This is fundamentally different from the destabilization of the HOMO determined upon substitution in **1-Me**. For **4** (Figure 3d) as well, the major change in the region 0−60° is found for the contribution from n_O-π, and this was the orbital identified as the cause of the shielding upon substitution. The n_O-$\pi/\pi^*_{C=O}$ mixing changes from HOMO−2/LUMO in the planar **4** to HOMO/LUMO+4 in the perpendicular **4**, with the HOMO being stabilized during the twist (Figure 4b). Overall, therefore, the deshielding from the n_O-π contribution decreases.

For **2** and **3**, the change in orbital contribution upon substitution was complex, and a specific orbital could not be identified as being responsible for the observed changes. In the torsional analyses, for **2** (Figure 3b), it is the n_O-σ contribution (△) that shows the largest overall change. The energetically low-lying n_O-σ expectedly does not have a deshielding contribution in the planar **2**, even though the n_O-$\sigma/\pi^*_{N=O}$ mixing is in

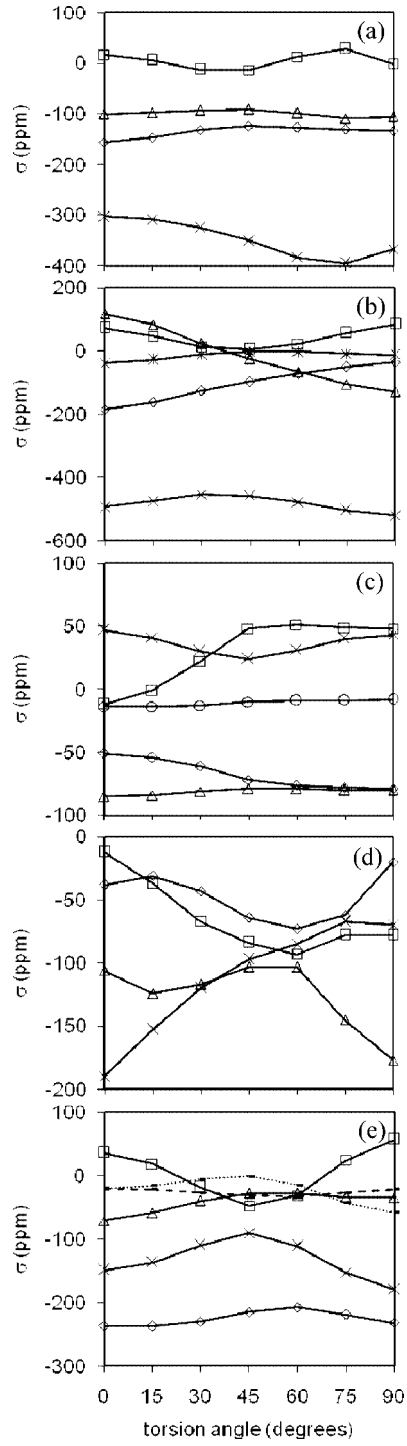

Figure 3. Dependence of orbital contributions to σ_{iso} on the torsion angle: (a) Ph−CHO (**1**), (b) Ph−NO_2 (**2**), (c) Ph−NCO (**3**), (d) Ph−$NHCOCH_3$ (**4**), and (e) Ph−NSO (**5**); (◇) σ_{X-O}, (□) $\pi_{X=O}$, (△) n_O-σ, (×) n_O-π, (∗) $\pi_{C=C}$, (○) σ_{N-C} of N═C; (- - -); n_S, (•••) n_N.

principle magnetically active. The reason for its deshielding contribution in the perpendicular **2** is similar to that discussed for **5-Bu** above (Chart 4), but the effect is more pronounced. The HOMO of the perpendicular **2** possesses large coefficients on oxygen in the NO_2 plane, which can mix with $\pi^*_{N=O}$ (LUMO). This σ-component, which is not present in the HOMO of the planar **2**, becomes more important as the torsion angle increases. For **3** (Figure 3c), it is the $\pi_{C=O}$ contribution (□) that dominates the change in σ_{iso}. For this contribution to be magnetically active, the in-plane $\pi_{C=O}$ has to mix with an unoccupied orbital perpendicular to the NCO plane that has a

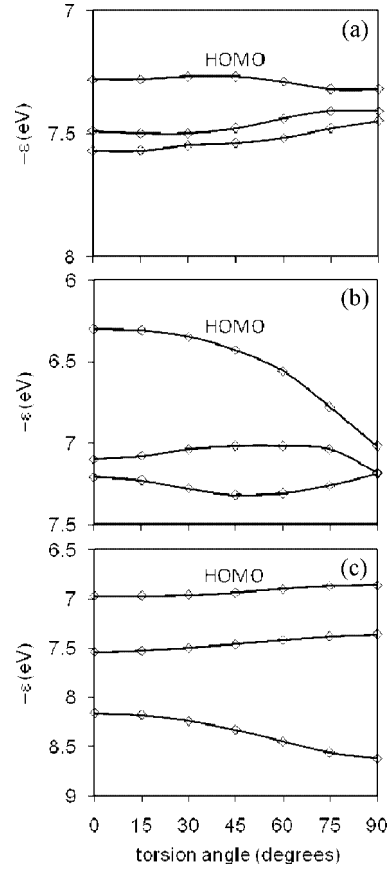

Figure 4. Dependence of orbital energies on the torsion angle: HOMO to HOMO−2 for (a) Ph−CHO (**1**), (b) Ph−$NHCOCH_3$ (**4**), and (c) Ph−NSO (**5**).

coefficient on oxygen. For the planar **3**, this is the LUMO, but for the twisted species, the LUMO oxygen coefficient is found increasingly in the NCO plane, and the perpendicular **3** does not possess a low-lying unoccupied orbital with the above requirements. The torsional analyses in parts b and c of Figure 3 also provide an explanation of why the orbital contributions for the substituted **2** and **3** were impossible to analyze (see above). A change of substituent, with its particular electronic and steric effects, can cause the stabilization or destabilization of each of the important molecular orbitals, resulting in a more or less important contribution to σ_{iso} and the nonuniform trends seen in Tables 2 and 3.

Finally, for **5** (Figure 3e), the n_O-π contribution (×) most accurately reflects the change in σ_{iso} (Figure 2e). But the changes from n_O-π are in fact overridden by those from $\pi_{S=O}$, and the overall change in σ_{iso}, i.e., the shielding up to 45° and the subsequent deshielding, is only reproduced when changes in n_O-π are augmented by those from n_O-σ (Δ) and n_N (dotted line). The importance of the n_O-π contribution was already apparent from Table 2, where it was overwhelming. For **5-Bu**, the deshielding observed was explained with an n_O-π-type contribution to the HOMO that was absent in **5** (Chart 4). The same holds here. For the planar **5**, n_O-π is HOMO−2, but an n_O-π-type contribution grows in the HOMO during the twist, notably from 60° on. Thus, while HOMO−2 is stabilized during the twist (Figure 4c), leading to the gain in shielding of n_O-π up to 45°, the contribution from the HOMO becomes increasingly important from 60° on, resulting in the loss in shielding.

4. Conclusions

We have presented calculations on the change in chemical shielding of the terminal oxygen atoms in five different

functional groups. The changes were studied upon substitution and torsion of aromatic aldehydes, nitro compounds, isocyanates, amides (acetanilides), and sulfinylamines (*N*-sulfinylanilines). The experimentally determined change in ^{17}O chemical shift upon substitution is accurately reproduced by the calculations, both in direction and in magnitude.

The change in charge of oxygen is often given as a reason for a change in chemical shift. The present study shows that for the small selection of molecules, the direction of change in σ_{iso} (deshielded or shielded) upon substitution is in general not dependent on the change in charge on oxygen, but when a torsion is forced without perturbing substituents on the aromatic ring, the change in charge is as expected from resonance arguments. Yet not a change in charge but changes in energies and alignments of molecular orbitals govern σ_{iso}. And because of this, the ^{17}O chemical shift is in principle not a good indicator for the size of torsion angles in substituted aromatic compounds with terminal oxygen atoms, as is shown for benzaldehydes and phenyl isocyanates. Even though the same shielding or deshielding than through substitution is found upon a relaxed torsional scan of the unsubstituted system (with the exception of *N*-sulfinylaniline), the effect cannot be used to infer torsion upon substitution. *N*-Sulfinylaniline, finally, shows a unique (for the systems studied here) behavior of σ_{iso} upon torsion with a maximum at 45°. This knowledge is expected to shed light onto the changes in ^{17}O chemical shift observed in our studies of *N*-sulfinylanilines and their complexes.

The oxygen nucleus is a fantastic reporter for its environment. Even here, for isolated molecules in the gas phase, free from outside interactions, environmental influences are reported according to changes in the mixing molecular orbitals. These changes range from straightforward to very complex, depending on the molecule, and to avoid misinterpretation of the experimental findings from ^{17}O NMR studies, it seems prudent to conduct detailed computational analyses when dealing with conformational effects that involve a terminal oxygen atom.

Acknowledgment. Calculations were performed at the Centre for Research in Molecular Modeling (CERMM), which was established with the financial support of the Concordia University Faculty of Arts and Science, the Ministère de l'Éducation du Québec (MEQ), and the Canada Foundation for Innovation (CFI). This work was supported by a research grant from the Natural Sciences and Engineering Research Council of Canada (NSERC).

References and Notes

(1) Boykin, D. W. *17O NMR Spectroscopy in Organic Chemistry*; CRC Press: Boca Raton, FL 1991 and references therein.
(2) Boykin, D. W. *Spectrosc. Lett.* **1987**, *20*, 415.
(3) Boykin, D. W.; Deadwyler, G. H.; Baumstark, A. L. *Magn. Reson. Chem.* **1988**, *26*, 19.
(4) Boykin, D. W.; Balakrishnan, P.; Baumstark, A. L. *Magn. Reson. Chem.* **1987**, *25*, 248.
(5) Balakrishnan, P.; Boykin, D. W. *J. Org. Chem.* **1985**, *50*, 3661.
(6) Brown, C. J. *Acta Crystallogr.* **1966**, *21*, 442.
(7) St. Amour, T. E.; Burgar, M. I.; Valentine, B.; Fiat, D. *J. Am. Chem. Soc.* **1981**, *103*, 1128.
(8) Cerioni, G.; Culeddu, N.; Plumitallo, A. *Tetrahedron* **1993**, *49*, 2957.
(9) Dahn, H.; Carrupt, P.-A. *Magn. Reson. Chem.* **1997**, *35*, 577.
(10) Liu, Y.; Nekvasil, H.; Tossell, J. *J. Phys. Chem. A* **2005**, *109*, 3060.
(11) Musio, R.; Sciacovelli, O. *Magn. Reson. Chem.* **2006**, *44*, 753.
(12) Mothana, B.; Ban, F.; Boyd, R. J.; Thompson, A.; Hadden, C. E. *Mol. Phys.* **2005**, *103*, 1113.
(13) Dahn, H. *J. Chem. Educ.* **2000**, *77*, 905.
(14) Pople, J. A.; Schneider, W. G.; Bernstein, H. J. *High-Resolution Nuclear Magnetic Resonance*; McGraw-Hill: New York, 1959.
(15) Karplus, M.; Pople, J. A. *J. Chem. Phys.* **1963**, *38*, 2803.
(16) Frisch, M. J.; Trucks, G. W.; Schlegel, H. B.; Scuseria, G. E.; Robb, M. A.; Cheeseman, J. R.; Zakrzewski, V. G.; Montgomery, J. A., Jr.; Stratmann, R. E.; Burant, J. C.; Dapprich, S.; Millam, J. M.; Daniels, A. D.; Kudin, K. N.; Strain, M. C.; Farkas, O.; Tomasi, J.; Barone, V.; Cossi, M.; Cammi, R.; Mennucci, B.; Pomelli, C.; Adamo, C.; Clifford, S.; Ochterski, J.; Petersson, G. A.; Ayala, P. Y.; Cui, Q.; Morokuma, K.; Salvador, P.; Dannenberg, J. J.; Malick, D. K.; Rabuck, A. D.; Raghavachari, K.; Foresman, J. B.; Cioslowski, J.; Ortiz, J. V.; Baboul, A. G.; Stefanov, B. B.; Liu, G.; Liashenko, A.; Piskorz, P.; Komaromi, I.; Gomperts, R.; Martin, R. L.; Fox, D. J.; Keith, T.; Al-Laham, M. A.; Peng, C. Y.; Nanayakkara, A.; Challacombe, M.; Gill, P. M. W.; Johnson, B.; Chen, W.; Wong, M. W.; Andres, J. L.; Gonzalez, C.; Head-Gordon, M.; Replogle, E. S.; Pople, J. A. *Gaussian 03*, revision C.02; Gaussian, Inc.: Wallingford, CT, 2004.
(17) Becke, A. D. *J. Chem. Phys.* **1993**, *98*, 5648.
(18) Lee, C.; Yang, W.; Parr, R. G. *Phys. Rev. B* **1988**, *37*, 785.
(19) Stephens, P. J.; Devlin, F. J.; Chabalowski, C. F.; Frisch, M. J. *J. Phys. Chem.* **1994**, *98*, 11623.
(20) Barone, V.; Cossi, M.; Tomasi, J. *J. Comput. Chem.* **1998**, *19*, 404.
(21) Barone, V.; Cossi, M.; Tomasi, J. *J. Chem. Phys.* **1997**, *107*, 3210.
(22) Cossi, M.; Barone, V.; Cammi, R.; Tomasi, J. *Chem. Phys. Lett.* **1996**, *255*, 327.
(23) Cohen, A. J.; Handy, N. C. *Mol. Phys.* **2001**, *99*, 607.
(24) Perdew, J. P.; Burke, K.; Ernzerhof, M. *Phys. Rev. Lett.* **1996**, *77*, 3865.
(25) Wu, A.; Zhang, Y.; Xu, X.; Yan, Y. *J. Comput. Chem.* **2007**, *28*, 2431.
(26) Schreckenbach, G.; Ziegler, T. *J. Phys. Chem.* **1995**, *99*, 606.
(27) Ditchfield, R. *Mol. Phys.* **1974**, *27*, 789.
(28) Wolinski, K.; Hinton, J. F.; Pulay, P. *J. Am. Chem. Soc.* **1990**, *112*, 8251.
(29) Klein, R. A.; Mennucci, B.; Tomasi, J. *J. Phys. Chem. A* **2004**, *108*, 5851.
(30) Bohmann, J. A.; Weinhold, F.; Farrar, T. C. *J. Chem. Phys.* **1997**, *107*, 1173.
(31) Reed, A. E.; Curtiss, L. A.; Weinhold, F. *Chem. Rev.* **1988**, *88*, 899.
(32) Bader, R. F. W. *Atoms in Molecules. A Quantum Theory*; Clarendon Press: Oxford, U.K., 1990.
(33) AIM2000, version 1.0. AIM2000 Home Page at http://www.aim2000.de (accessed on August 12, 2008).
(34) Portmann, S.; Lüthi, H. P. *Chimia* **2000**, *54*, 766.
(35) Flükiger, P.; Lüthi, H. P.; Portmann, S.; Weber, J. *MOLEKEL 4.3*; Swiss Center for Scientific Computing: Manno, Switzerland, 2000−2002.
(36) Borisenko, K. B.; Bock, C. W.; Hargittai, I. *J. Phys. Chem.* **1996**, *100*, 7426.
(37) Kakar, R. K.; Rinehart, E. A.; Quade, C. R.; Kojima, T. *J. Chem. Phys.* **1970**, *52*, 3803.
(38) See, e.g., Gdaniec, M.; Ibragimov, B. T.; Talipov, S. A. *Acta Crystallogr., Sect. C: Cryst. Struct. Commun.* **1991**, *47*, 573.
(39) Braude, E. A.; Sondheimer, F. *J. Chem. Soc.* **1955**, 3754.
(40) Moorthy, J. N.; Mal, P.; Natarajan, R.; Venugopalan, P. *J. Org. Chem.* **2001**, *66*, 7013.
(41) St. Amour, T. E.; Burgar, M. I.; Valentine, B.; Fiat, D. *J. Am. Chem. Soc.* **1981**, *103*, 1128.
(42) Dahn, H.; Péchy, P.; Toan, V. V. *Magn. Reson. Chem.* **1997**, *35*, 589.
(43) Jensen, F. *Introduction to Computational Chemistry*, 2nd edition; Wiley: Chichester, U.K., 2007.
(44) Høg, J. H.; Nygaard, L.; Sorensen, G. O. *J. Mol. Struct.* **1970**, *7*, 111.
(45) Dorofeeva, O. V.; Vishnevskiy, Y. V.; Vogt, N.; Vogt, J.; Khristenko, L. V.; Krasnoshchekov, S. V.; Shishkov, I. F.; Hargittai, I.; Vilkov, L. V. *Struct. Chem.* **2007**, *18*, 739.
(46) Domenicano, A.; Schultz, G.; Hargittai, I.; Colapietro, M.; Portalone, G.; George, P.; Bock, C. W. *Struct. Chem.* **1990**, *1*, 107.
(47) Shishkov, I. F.; Sadova, N. I.; Novikov, V. P.; Vilkov, L. V. *Zh. Strukt. Khim.* **1984**, *25*, 98.
(48) Trotter, J. *Acta Crystallogr.* **1959**, *12*, 884.
(49) Boese, R.; Bläser, D.; Nussbaumer, M.; Krygowski, T. M. *Struct. Chem.* **1992**, *3*, 363.
(50) Trotter, J. *Acta Crystallogr.* **1959**, *12*, 605.
(51) Bouchy, A.; Roussy, G. *C. R. Acad. Sci., Ser. C* **1973**, *277*, 143.
(52) Dahn, H.; Péchy, P.; Carrupt, P.-A. *Magn. Reson. Chem.* **1996**, *34*, 283.
(53) Wasserman, H. J.; Ryan, R. R.; Layne, S. P. *Acta Crystallogr., Sect. C: Cryst. Struct. Commun.* **1985**, *41*, 783.
(54) Johnson, S. W.; Eckert, J.; Barthes, M.; McMullan, R. K.; Muller, M. *J. Phys. Chem.* **1995**, *99*, 16253.
(55) Manea, V. P.; Wilson, K. J.; Cable, J. R. *J. Am. Chem. Soc.* **1997**, *119*, 2033.
(56) Caminati, W.; Maris, A.; Millemaggi, A. *New J. Chem.* **2000**, *24*, 821.
(57) Ullrich, S.; Müller-Dethlefs, K. *J. Phys. Chem. A* **2002**, *106*, 9181.

(58) Ilieva, S.; Hadjieva, B.; Galabov, B. *J. Org. Chem.* **2002**, *67*, 6210.
(59) Hanson, J. R.; Hitchcock, P. B.; Rodriguez-Medina, I. C. *J. Chem. Res.* **2004**, 664.
(60) Smith, W. T., Jr.; Trimnell, D.; Grinninger, L. D. *J. Org. Chem.* **1959**, *24*, 664.
(61) Meij, R.; Oskam, A.; Stufkens, D. J. *J. Mol. Struct.* **1979**, *51*, 37.
(62) Caminati, W.; Mirri, A. M.; Maccagnani, G. *J. Mol. Spectrosc.* **1977**, *66*, 368.
(63) Romano, R. M.; Della Védova, C. O.; Boese, R. *J. Mol. Struct.* **1999**, *475*, 1.
(64) Romano, R. M.; Della Védova, C. O.; Hildebrandt, P. *J. Mol. Struct.* **1999**, *508*, 5.
(65) Muchall, H. M. *J. Phys. Chem. A* **2001**, *105*, 632.
(66) Iwasaki, F. *Acta Crystallogr., Sect. B: Struct. Crystallogr. Cryst. Chem.* **1980**, *36*, 1700.
(67) Dahn, H.; Pechy, P.; Toan, V. V.; Bonini, B. F.; Lunazzi, L.; Mazzanti, G.; Cerioni, G.; Zwanenburg, B. *J. Chem. Soc., Perkin Trans. 2* **1993**, 1881.
(68) Penner, G. H.; George, P.; Bock, C. W. *J. Mol. Struct.: THEOCHEM* **1987**, *152*, 201.
(69) See, e.g., Sancho-García, J. C.; Pérez-Jiménez, A. J. *J. Chem. Phys.* **2003**, *119*, 5121.
(70) Bouchy, A.; Roussy, G. *J. Mol. Spectrosc.* **1977**, *65*, 395.

JP804670H